Am J Transl Res 2025;17(2):1223-1236
www.ajtr.org /ISSN:1943-8141/AJTR0158103

Original Article

TIGAR alleviates cognitive impairment in rats with chronic cerebral hypoperfusion by suppressing oxidative stress and pyroptosis

Jie Xiao[1,2], Min Wu[1,2], Hailong Li[2,3], Shufan Zhang[1,2], Jing Deng[1,2], Bihua Wu[1]

[1]*Department of Internal Medicine, Nanchong Mental Health Center, Nanchong 637000, Sichuan, China;* [2]*Innovation Centre for Science and Technology, North Sichuan Medical College, Nanchong 637000, Sichuan, China;* [3]*Department of Gastroenterology, Wusheng People's Hospital, Guang'an 638500, Sichuan, China*

Received May 28, 2024; Accepted January 18, 2025; Epub February 15, 2025; Published February 28, 2025

Abstract: Background: It is postulated that oxidative stress and pyroptosis, which are induced by chronic cerebral hypoperfusion (CCH), contribute to the pathogenesis of vascular cognitive impairment (VCI). The protective role of TIGAR in neurologic illnesses has been the subject of extensive examination, yet its role in models of CCH-induced cognitive impairment remains unexplored. The objective of this study was to ascertain whether TIGAR is a neuroprotective agent in rats with CCH that reduces oxidative stress and pyroptosis. Methods: A CCH model was established in rats through the use of bilateral common carotid artery occlusion (BCCAO). The effects of TIGAR on cognitive function and anxiety-depressive behaviors in rats with CCH were examined. To this end, the Y-maze and open field tests were employed. Nissl and hematoxylin-eosin (H&E) staining were used to assess histologic changes in the CA1 area of the hippocampus. Hippocampal glutathione (GSH) activity, malondialdehyde (MDA) content, and NADPH/NADP+ ratio were measured using the WST-8 colorimetric method to assess oxidative stress. The expression of TIGAR and pyroptosis-related proteins was assessed by western blotting. Results: A model of CCH-induced cognitive impairment was successfully established. Four weeks after BCCAO, cerebral blood flow returned to normal in the rats, and cognitive impairment and anxiety-depression-like behavior developed. In rats with CCH, MDA levels increased, GSH activity and NADPH/NADP+ ratio decreased, and pyroptosis-related protein expression increased. The pathologic findings indicated that there was an exacerbation of neuronal injury in the CA1 area of the hippocampus and that the cells were loosely arranged. In rats with CCH, overexpression of TIGAR reduced pyroptosis-associated protein expression while increasing MDA content, GSH activity, and NADPH/NADP+ ratio. It promoted neuronal cell survival, and improved cognitive function and anxiety-depression-like behavior. Conclusion: Overexpression of TIGAR reduced CCH-induced oxidative stress and pyroptosis and ameliorated cognitive dysfunction and anxiety-depression-like behavior in rats. These findings suggest that TIGAR counteracts oxidative stress and prevents pyroptosis, making it a promising target for the treatment of VCI.

Keywords: TIGAR, oxidative stress, pyroptosis, BCCAO

Introduction

Vascular cognitive impairment (VCI) refers to any level of cognitive decline induced by cerebrovascular disease, including the entire process from subjective cognitive decline to dementia [1]. Its prevalence is second only to Alzheimer's disease (AD) in terms of the number of people with dementia. Currently, there is no specific drug for the treatment of VCI. Therefore, research is needed into the underlying molecular mechanisms of VCI and the development of new drugs.

Chronic cerebral hypoperfusion (CCH) is a major cause of the clinical manifestations of VCI [2]. The onset and development of nerve damage and cognitive dysfunction caused by CCH are associated with oxidative stress and pyroptosis [3, 4]. Pyroptosis is a type of programmed cell death characterized by inflammation that can be triggered by the accumulation of reactive oxygen species (ROS). During ischemic-hypoxic brain injury, intracellular mitochondrial dysfunction leads to the production of excess ROS, which stimulates the formation of the NLRP3 inflammasome and activates caspase-1 [5]. On

https://doi.org/10.62347/NWQS1671

the one hand, activated caspase-1 cleaves the target protein GSDMD to GSDMD-NT, resulting in cell membrane leakage. On the other hand, pro-IL-1β and pro-IL-18 are enzymatically cleaved to mature IL-1β and IL-18, which are subsequently released through the cell membrane pores, a prominent feature of pyroptosis [6].

TP53-induced glycolysis and apoptosis regulator (TIGAR) is a downstream target gene of p53 located in organelles and the cytoplasm. TIGAR is structurally and functionally similar to fructose-2,6-diphosphatase and performs enzymatic functions by reducing fructose-2,6-diphosphate to inhibit glycolysis and lower intracellular ROS levels [7]. TIGAR has been demonstrated to exert neuroprotective effects in the context of cerebral ischemia/reperfusion injury, with a concomitant reduction in ROS levels [8]. In addition, in a study of gestational diabetes, loss of TIGAR was shown to increase intracellular ROS accumulation and stimulate caspase-1-dependent pyroptosis [9]. This suggested that TIGAR protects against VCI induced by CCH by reducing ROS and inhibiting pyroptosis.

A cognitive impairment model induced by CCH was successfully created four weeks after bilateral common carotid artery occlusion (BCCAO) in this study. The expression level of TIGAR in the hippocampus was measured to investigate the neuroprotective effect and mechanism of TIGAR overexpression in a CCH model [10].

Materials and methods

Animals

The Laboratory Animal Center of North Sichuan Medical College provided male Sprague-Dawley rats with a weight range of 210 to 250 grams and an age range of 6 to 8 weeks. The rats were housed in standard conditions prior to the experiment, with a temperature of 22°C, a humidity of 60%, and a 12-hour cycle of light and dark (from 08:30 to 20:30 during the light period). Additionally, the rats had unrestricted access to food and water. The research was carried out following the guidelines stated in the Chinese Guidelines for the Utilization of Laboratory Creatures and the National Institutes of Health (NIH) Guidelines for the Treatment and Utilization of Laboratory Creatures. It was approved by the Ethics Committee for Animal Experiments of North Sichuan Medical College (Ethics No. [2023] 020). At the end of the experiment, the rats were painlessly euthanized under anesthesia by inhalation of excessive amounts of isoflurane, ensuring animal welfare and minimizing suffering.

Rat model of CCH

The BCCAO model is the most commonly utilized method for preparing CCH. The rats were intraperitoneally injected with 1% pentobarbital (50 mg/kg) and subsequently fixed on the operating table after achieving full anesthesia. During the procedure, the neck skin was disinfected and a 1 cm incision was made along the midabdominal line. With great care, the underlying layer of skin was meticulously incised to expose both sides of the common carotid artery (CCA). The vagus nerve was then meticulously detached from the CCA with a glass rod. One side of the CCA was occluded, and the other side of the CCA was ligated after 15 minutes.

Cerebral blood flow

Following anesthesia and fixation of the rats, a high-speed electric drill was employed to gradually polish the skull until it reached the desired thickness. Blood flow was observed under a speckle imaging system (SIM BFI HR Pro, Wuhan, China), with one image recorded every 1 second, resulting in 10 consecutive blood flow distribution maps. These were then subjected to statistical analysis. Subsequently, the blood flow distribution map was recorded, and the surgical outcome was evaluated by comparing the mean blood flow in the region of interest (ROI) before and after the procedure.

Virus injection

TIGAR high-expression adeno-associated viruses and control viruses, named AAV-TIGAR and AAV-NC, respectively, were customized and purchased from Obio Technology Co., Ltd. (Shanghai, China). After general anaesthesia with 1% pentobarbital, the rat brain was immobilised using a stereoscope (Stoelting, USA), the hair on the top of the head was removed, the skin was cut with ophthalmic scissors to exposed the skull, and the cranial cavity was drilled with a cranial drill. The hippocampus was injected with 1.5 μl of virus using a 5 μl

Hamilton microliter syringe at a rate of 0.1 μl/min (coordinates from bregma: AP=-3.6 mm, ML=±2.8 mm, DV=-3.5 mm). After each injection, the needle was left in place for 10 minutes and then removed slowly and evenly. After bilateral virus injection was completed, the rats were fed normally for 3 weeks until the peak virus transfection was reached in subsequent experiments. The bilateral hippocampal expression of green fluorescent protein (GFP) was used as a marker of successful transfection of the corresponding viruses.

Experimental scheme

In accordance with the experimental design, the study was divided into two parts. In the first part, SD rats were randomly allocated into four groups: a sham group, a CCH1 group (2 weeks), a CCH2 group (3 weeks), and a CCH3 group (4 weeks) (n=4 for each group). The CA1 region of the hippocampus was collected, and TIGAR expression was detected in each group. In the second part, the rats were divided into a sham group, a CCH group, a CCH+AAV-TIGAR group and a CCH+AAV-NC group (n=10 for each group). The CCH+AAV-TIGAR and CCH+AAV-NC groups received AAV-TIGAR and AAV-NC virus injections, respectively. The sham group and the CCH group received the same dose of normal saline injection. Bilateral CCA ligation was performed 3 weeks later, and the sham group underwent the same operation without ligation of the CCA. After 4 weeks, each group underwent behavioral tests, and brain tissue was collected for pathologic and molecular biological examination.

Behavioral tests

Twenty-eight days following the surgical procedure, the rats were evaluated. The Y-maze test (Clever Sys. Inc./Topscan USA) was a test of spontaneous variation conducted in a Y-shaped maze with three arms that were comparable in length and angle. Mice with no cognitive impairment might recall sections of the previous maze and could naturally explore parts of the Y-shaped maze that had never been visited before. The camera system records the animal's behavior for a five-minute period, documenting the complete list of arm entries and the order of entry to ascertain the percentage of variation. The open field test was conducted over a period of 10 minutes, during which the activity of the animals was recorded. To facilitate the analysis of the data, the entire region was divided into sixteen identical sections. Each rat was positioned meticulously at the center of the field and observed for a period of ten minutes. Subsequently, the distance traversed while walking, the frequency of movement, and the duration of stay within the central region were documented. To eliminate any residual odor, the test gap was gently rubbed and the bottom of the box was meticulously cleaned with a solution of 50% ethanol.

Histologic evaluation

Ischemic changes in neurons required histologic evaluation. Under general anesthesia, 0.9% normal saline was injected through the heart and 4% paraformaldehyde was reinjected to fix the brain. The brain was removed from the skull and immersed in 4% paraformaldehyde for 4-6 h. The sections were dehydrated and then embedded in paraffin for embedding. The brain was cut into 2-μM thick coronal sections using a microtome (Leica, Germany) and mounted on a microscope slide. The distribution of neurons in the rat hippocampus was observed under a microscope using standard hematoxylin-eosin (H&E) staining (Servicebio, China). Nissl bodies in the brains of rats were detected by Nissl staining (Solarbio, China).

Transmission electron microscopy

A total of 1 mm^3 of hippocampal tissue was extracted and preserved in 2.5% glutaraldehyde at 4°C overnight. A 1% solution of osmic acid was then applied to the sample at room temperature for two hours. The tissue was then washed three times for 15 minutes each with 0.1 M phosphate-buffered saline (pH 7.4). After removal of water with various concentrations of acetone, the tissues were immersed in resin, cut into ultrathin sections (70-90 nm), and then treated with uranyl acetate and lead citrate for staining. The sections were then analyzed using a transmission electron microscope (H7650, Hitachi, Japan).

Western blotting

After the hippocampal tissue was obtained, the tissue was homogenized in lysis buffer (RIPA) containing protease and phosphorylase inhibitors (ServiceBio, China) and centrifuged at low

temperature (12,000 rpm, 10 min, 4°C) to collect the supernatant. The BCA kit (Beyotime Biotechnology, China) was used to determine the protein concentration of each sample. Proteins were separated by polyacrylamide gel electrophoresis (SDS-PAGE) and electrotransferred to PVDF membrane. Sections were blocked with 5% skim milk for 2 hours at room temperature and then exposed to primary antibody overnight in a refrigerator set at 4°C. The following primary antibodies were used: TIGAR (1:1,000 ab189164 Abcam), NLRP3 (1:1,000 265863 MCE), Cleaved-Caspase-1 (1:1,000 263712 MCE), GSDMD-NT (1:1,000 H600-010005 HUABIO), and IL-1β (1:1,000 263418 MCE). The membrane was incubated with the secondary antibody for 1 hour at room temperature after three washes with TBST on the second day. A chemiluminescence system (OriGene, USA) was used to visualize protein bands, and Image (NIH, Bethesda, Maryland, USA) was used for gray scale analysis.

Oxidative stress evaluation

Hippocampal samples were homogenized with PBS at 4°C and then centrifuged at 12,000×g for 10 minutes at 4°C. The extracted supernatant was then collected.

The protein concentration in each specimen was determined by the BCA method. To determine MDA, T-Hippocampal glutathione (GSH), GSSG, NADPH, and total NADP+ activity, the MDA colorimetric assay kit, T-GSH/GSSG colorimetric assay kit, and NADPH/NADP+ colorimetric assay kit (Elabscience, China) were employed.

The protein content of each sample was then normalized. GSH=T-GSH-2×GSSG. NADPH/NADP+=NADPH/([NADP]total-NADPH) ×100%.

Statistical analysis

Statistical analysis was performed using SPSS 22.0 software. Group differences were compared by one-way analysis of variance. The LSD test was performed for data with equal differences. Statistical significance was set at $P<0.05$, and data were presented as mean ± SEM. All data were first tested for normal distribution and homogeneity of variance. For data satisfying normal distribution and homogeneity of variance, one-way analysis of variance (ANOVA) followed by Tukey's HSD multiple comparison test was used for inter-group comparisons. For data that did not meet these conditions, inter-group comparisons were performed using the Kruskal-Wallis test, followed by multiple comparison correction using Dunn's test. All tests were two-tailed and the significance level was set at $P<0.05$. The effect size (Cohen's d) was also calculated for each T-test to assess the magnitude of the treatment effect. For all ANOVA analyses, Levene's test for homogeneity of variance was performed to ensure that the data met the requirements for ANOVA. For data that did not satisfy homogeneity of variance, Welch's ANOVA was used. In all cases, the raw data and the choice of statistical test are detailed in the legend or main text of each experiment.

Results

Increased TIGAR expression in hippocampal tissue of CCH rats

The study used BCCAO to establish a CCH model and monitored cerebral blood flow (CBF) in rats using a speckle imaging system (**Figure 1A**). CBF decreased immediately after surgery and basically returned to baseline at 4 weeks, at which time many neovascular branches were observed (**Figure 1B**, **1C**). Western blot analysis showed a gradual increase in TIGAR expression in the hippocampal area of rats 3-4 weeks after BCCAO surgery ($P<0.05$, $P<0.001$; **Figure 1D**, **1E**). These results indicated that TIGAR was significantly activated in the CCH model.

Overexpression of TIGAR improved cognitive dysfunction and anxiety-depression-like behavior in rats with CCH

For investigation of the behavioral effect of TIGAR on rats with CCH, AAV-TIGAR or AAV-NC was injected into both sides of the hippocampus using stereotactic techniques.

The hippocampus showed evidence of substantial viral transfection (**Figure 2A**, **2B**). TIGAR expression was determined by western blotting for TIGAR (**Figure 2C**). The AAV-TIGAR+CCH group had higher TIGAR protein levels than the CCH group (**Figure 2D**, $P<0.05$), whereas there was no difference between the AAV-NC+CCH group and the CCH group. The exploratory and spatial memory abilities of the rats were

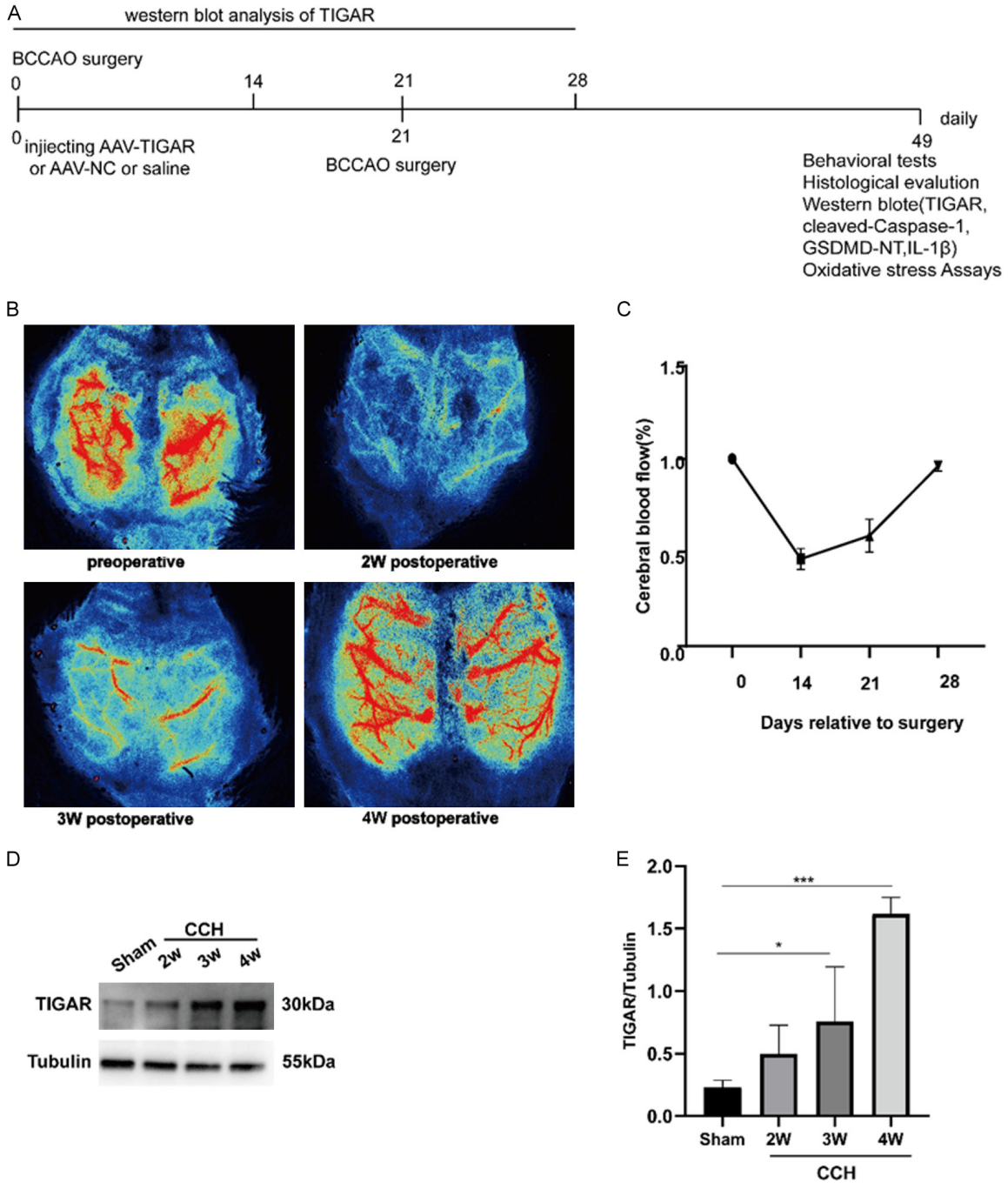

Figure 1. The rat CCH model was established, and the expression levels of TIGAR in the hippocampus after BCCAO are shown. A. Study design. B. Different time CBF following BCCAO. C. Quantification of relative CBF in ROI; n=10; D. Protein bands of temporal expression of TIGAR following BCCAO. E. Quantitative protein analysis of TIGAR. Data are expressed as the mean ± SEM (n=4, **P*<0.05, ****P*<0.001).

assessed using the Y-maze test (**Figure 3A**). The spontaneous alternation rate of rats in the CCH group was significantly decreased compared to that of the sham group (**Figure 3B**, *P*<0.001). After elevation of TIGAR levels, the rats exhibited a higher rate of spontaneous alternation compared to the CCH group (**Figure 3B**, *P*<0.001). However, no significant difference was observed between the AAV-NC+CCH group and the CCH group. Given the potential correlation between anxious and depressive-like behaviors and cognitive impairment, the

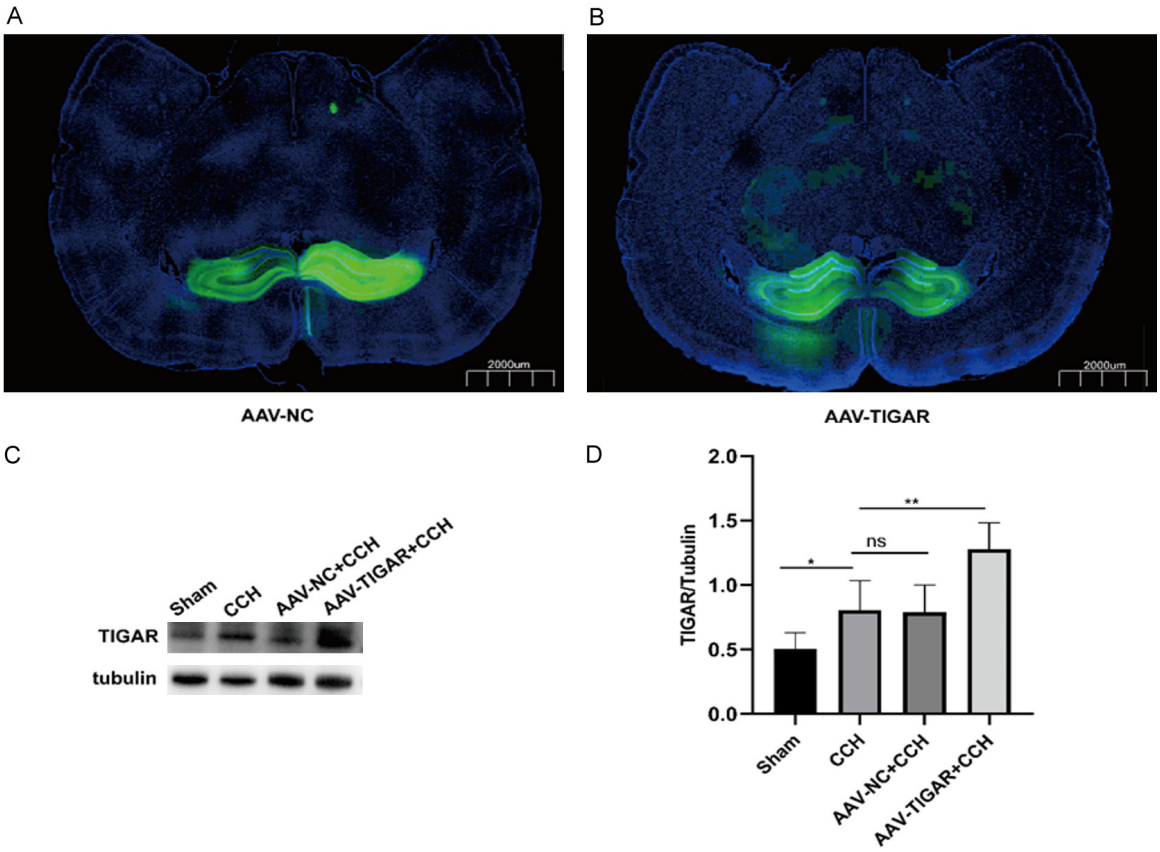

Figure 2. AAV-TIGAR or AAV-NC was injected into the bilateral hippocampal area of the SD rat. A. GFP expression of AAV-NC in the hippocampal area. B. GFP expression of AAV-TIGAR in the hippocampal area. C. Western blot showing protein expression of TIGAR. D. Statistical graph of grayscale values of TIGAR protein expression. Scale bar=2000 μm. Data are expressed as the mean ± SEM (n=5, **P*<0.05, ***P*<0.01, "ns" indicates *P*>0.05).

OFT was conducted. In the sham group, the central walking distance, residence time, and number of crossings were considerably higher compared to the CCH group (**Figure 3C-F**, *P*<0.001). The AVV-TIGAR+CCH group had significantly greater walking distance, dwell time, and number of crossings in the central area compared to the CCH group (**Figure 3C-F**, *P*<0.001). Neither AAV-NC+CCH nor CCH groups showed significant differences. These results showed that rats with CCH exhibited anxiety-depression-like behavior and cognitive impairment, and that these behaviors could be ameliorated in rats with CCH by overexpressing TIGAR.

Overexpression of TIGAR attenuates neuronal injury in rats with CCH

H&E and Nissl staining were performed on hippocampal slices to examine the pathologic damage to neurons in rats with CCH. Pyramidal cells of rats in the sham group were neatly arranged, the nuclear membrane was unbroken, and the nuclei were lightly stained according to H&E staining (**Figure 4A**). Pyramidal cells with deep staining and deviation of the nucleolus, irregular shape, blurred internal structure, decreased cell number, and thinning of the cell layer were clearly pathologically altered in the CCH group. The AAV-NC+CCH group showed no significant difference from the CCH group. The AAV-NC+CCH group was not significantly different from the CCH group. However, the AAV-TIGAR+CCH group showed reduced cell damage, relatively ordered pyramidal cell organization, and reduced nuclear fission and pyknosis. Furthermore, Nissl staining (**Figure 4B**) showed that the CCH group had significantly fewer hippocampal neurons and Nissl bodies than the sham group. The AVV-TIGAR+CCH group showed a significant increase in the number of hippocampal neurons compared to the CCH group. Comparable results were observed when Nissl-positive cells were counted (**Figure 4C**). These results suggest that TIGAR overex-

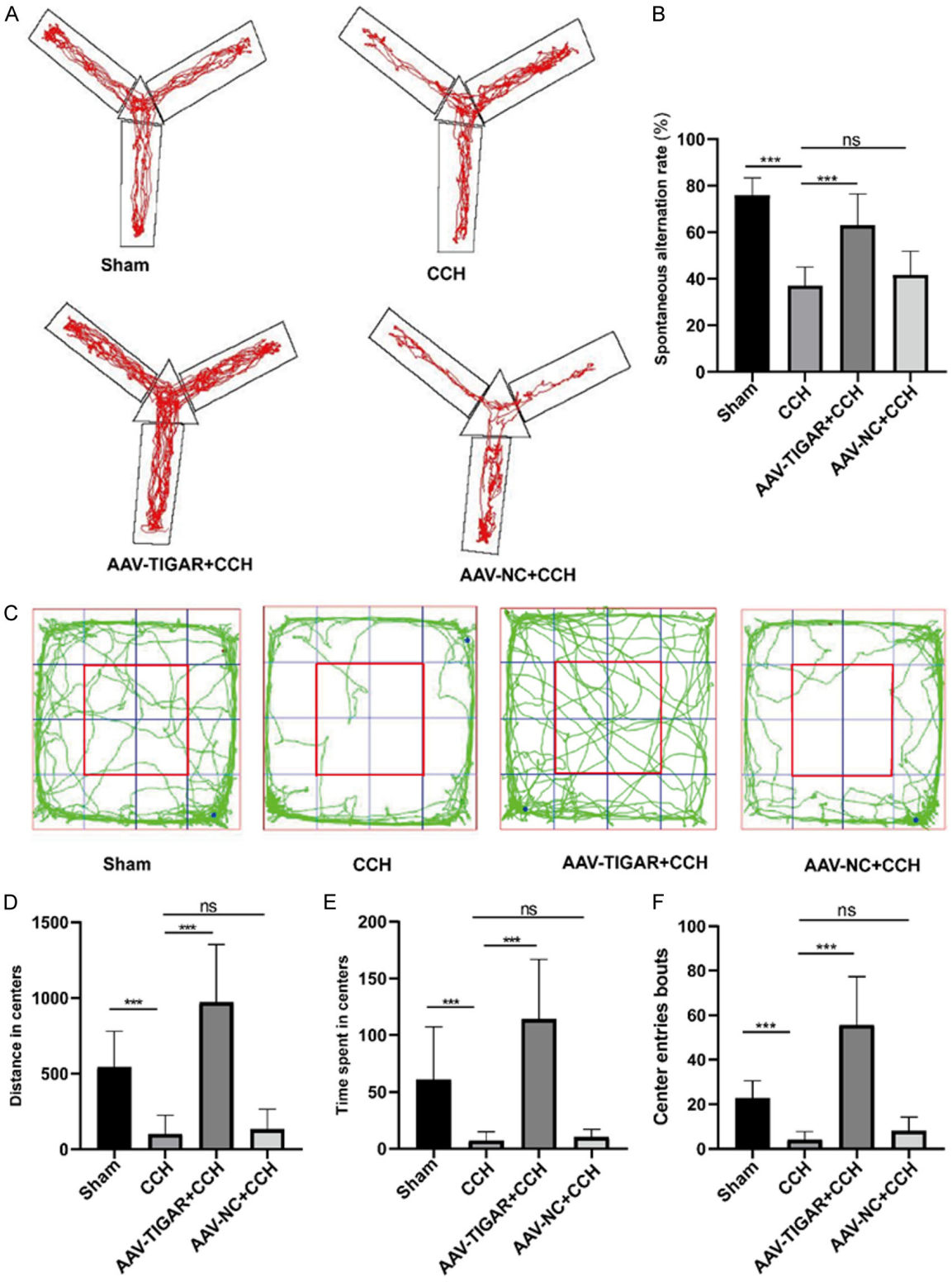

Figure 3. TIGAR protein overexpression alleviated cognitive dysfunction, anxiety, and depression in rats. A. Representative movement trajectories of rats in the Y-maze test. B. Spontaneous alternation rate of each group in the Y-maze test. C. Representative movement trajectories of rats in the OFT. D. Distance to the centers of each group in the OFT. E. Time spent in the centers for each group in the OFT. F. Center entries of each group in the OFT. Data are expressed as the mean ± SEM (n=8-10, ***P<0.001, "ns" indicates P>0.05).

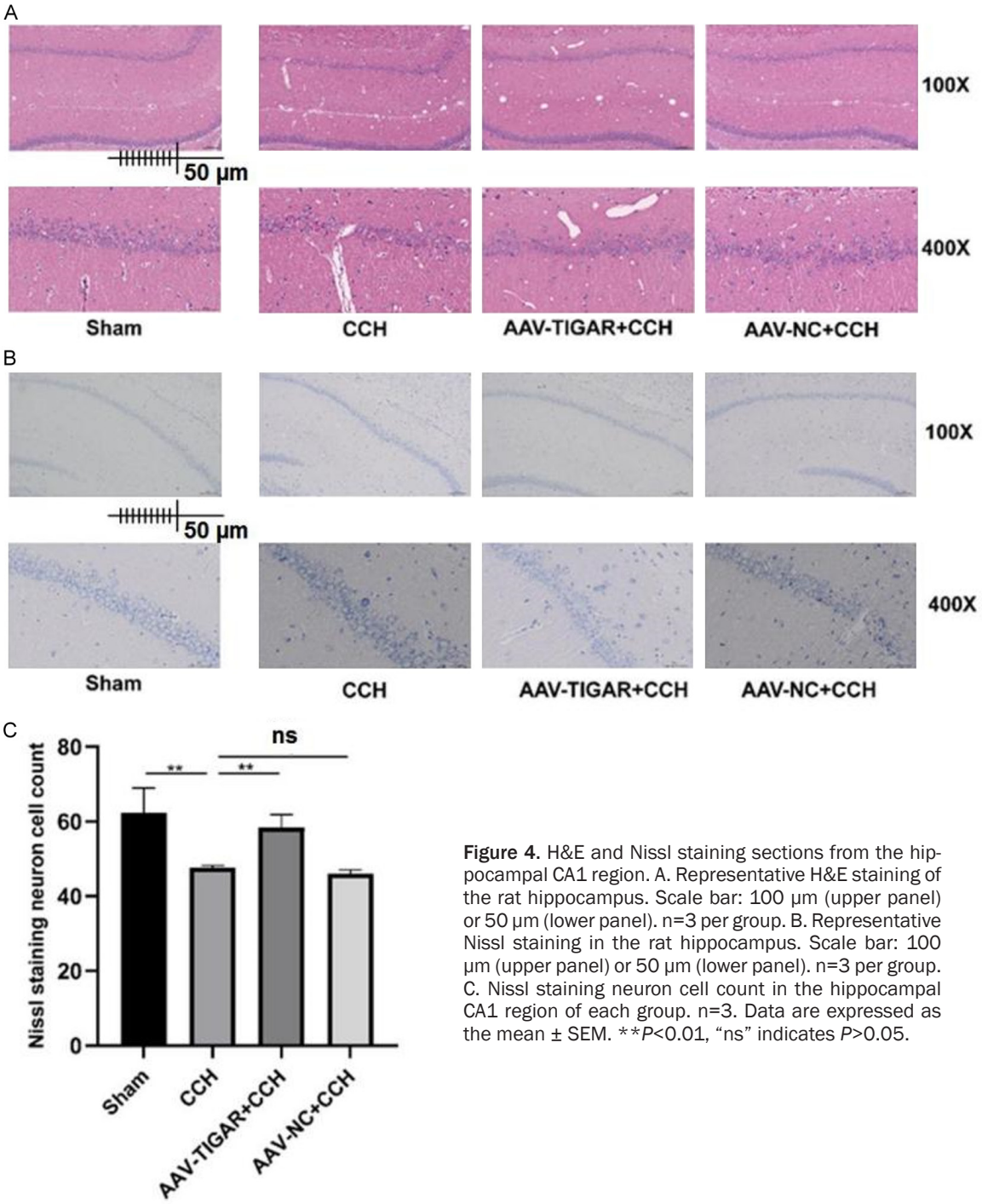

Figure 4. H&E and Nissl staining sections from the hippocampal CA1 region. A. Representative H&E staining of the rat hippocampus. Scale bar: 100 μm (upper panel) or 50 μm (lower panel). n=3 per group. B. Representative Nissl staining in the rat hippocampus. Scale bar: 100 μm (upper panel) or 50 μm (lower panel). n=3 per group. C. Nissl staining neuron cell count in the hippocampal CA1 region of each group. n=3. Data are expressed as the mean ± SEM. ***P*<0.01, "ns" indicates *P*>0.05.

pression can ameliorate the morphologic damage to neurons in rats with CCH.

Overexpression of TIGAR reduced oxidative stress in rats with CCH

Previous studies indicated that TIGAR had a protective effect on ischemic brain injury, and its mechanism was related to the reduction of oxidative stress injury [8]. The CCH group showed a significantly higher MDA level compared to the sham group (**Figure 5C**, *P*<0.01). The MDA level in the AVV-TIGAR+CCH group was lower than that of the CCH group (**Figure 5C**, *P*<0.001). The expression of MDA did not show any significant change from the AAV-

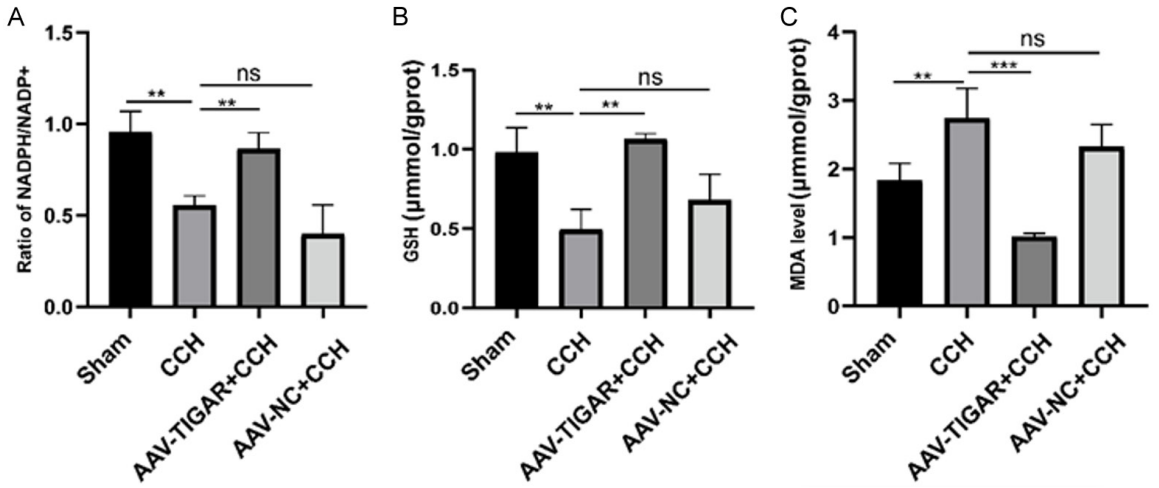

Figure 5. Overexpression of TIGAR attenuates oxidative stress in rats with CCH. A. NADPH/NADP+ ratios in the hippocampi of each group. B. Levels of GSH in the hippocampus of each group. C. Levels of MDA in the hippocampus of each group. Data are expressed as the mean ± SEM (n=3. ***P*<0.01, ****P*<0.001. "ns" indicates *P*>0.05).

NC+CCH group to the CCH group. In addition, the CCH group had significantly lower levels of GSH (**Figure 5B**, *P*<0.01) and NADPH/NADP+ (**Figure 5A**, *P*<0.01) than the sham group. Overexpression of TIGAR restored the expression levels of GSH (**Figure 5B**, *P*<0.01) and NADPH/NADP+ (**Figure 5A**, *P*<0.01). Furthermore, no significant difference was observed between the AAV-NC+CCH group and the CCH group. These results suggest that overexpression of TIGAR prevents CCH-induced oxidative stress by increasing the levels of antioxidant enzymes and decreasing the production of ROS.

Overexpression of TIGAR reduces focal cell death in CCH rats

The cognitive impairment observed in rats with CCH was related to pyroptosis [4]. To ascertain whether TIGAR played a role in pyroptosis in rats with CCH, the expression of key molecules involved in pyroptosis was detected. **Figure 6A-E** showed that in the CCH group, the levels of NLRP3 (*P*<0.01), GSDMD-NT (*P*<0.01), IL-1β (*P*<0.01), and cleaved caspase-1 (*P*<0.05) were higher than those of the sham group. After overexpression of TIGAR, the expression of NLRP3 (*P*<0.001), GSDMD-NT (*P*<0.05), IL-1β (*P*<0.01), and cleaved caspase-1 (*P*<0.001) decreased compared with those of the CCH group, but the AAV-NC+CCH group did not show any discernible difference from the CCH group. Pyroptosis is a type of cell death characterized by the formation of pores in the membrane induced by GSDMD, leading to cell lysis. To ascertain the impact of CCH on the neuronal membrane, transmission electron microscopy (TEM) was utilized. As shown in **Figure 6F**, the number of membrane holes in hippocampal neurons of rats with CCH was significantly increased, and the abnormalities were alleviated by overexpression of TIGAR. These results also supported the view that CCH induced neuronal pyroptosis and showed that overexpression of TIGAR can ameliorate the significance of CCH-induced neuronal pyroptosis.

Discussion

The objective of this study was to investigate the protective impact of TIGAR in a CCH rat model and its mechanism of action. To this end, a CCH rat model was created using BCCAO surgery. It was found that in the CCH rat model, oxidative stress was increased in the ischemic hippocampus. Furthermore, pyroptosis, which was mediated by the NLRP3 inflammasome, resulted in neuronal damage. It ultimately caused cognitive impairment in rats exhibiting anxiety and depression-like behavior. Overexpression of TIGAR can reduce the above CCH-induced damage. These results demonstrated the importance of TIGAR in protecting rat hippocampal neurons from injury under conditions of chronic cerebral ischemia.

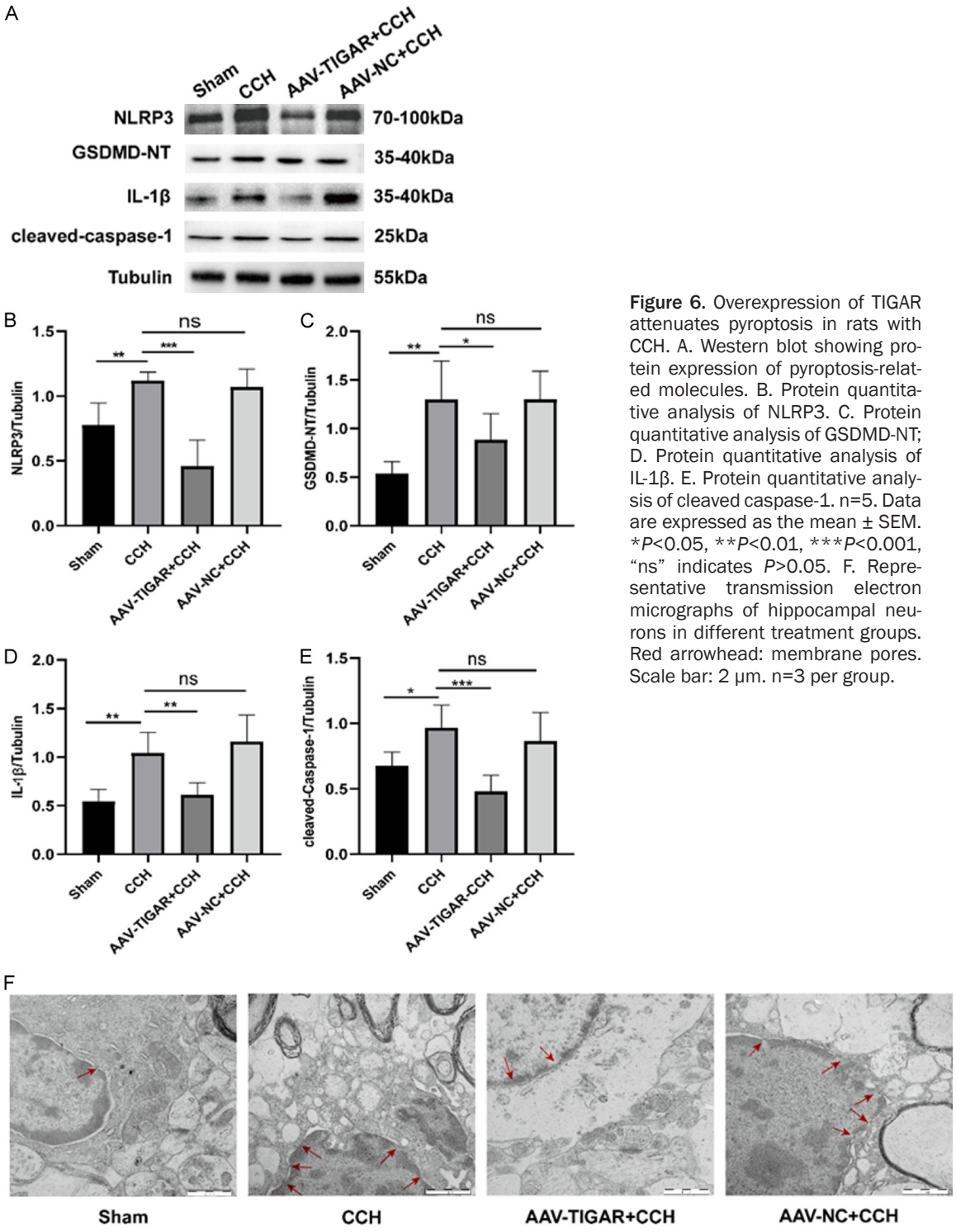

Figure 6. Overexpression of TIGAR attenuates pyroptosis in rats with CCH. A. Western blot showing protein expression of pyroptosis-related molecules. B. Protein quantitative analysis of NLRP3. C. Protein quantitative analysis of GSDMD-NT; D. Protein quantitative analysis of IL-1β. E. Protein quantitative analysis of cleaved caspase-1. n=5. Data are expressed as the mean ± SEM. **P*<0.05, ***P*<0.01, ****P*<0.001, "ns" indicates *P*>0.05. F. Representative transmission electron micrographs of hippocampal neurons in different treatment groups. Red arrowhead: membrane pores. Scale bar: 2 μm. n=3 per group.

CCH is defined as a continuous decrease in CBF caused by various cerebrovascular diseases and hemodynamic and hemodynamic changes [11]. The energy storage capacity of the brain is limited, and a reduction in CBF can lead to pathologic damage to the central nervous system, which is considered to be the core cause of VCI progression [12]. The CBF of VCI patients has been reported to be significantly lower than that of age-matched controls, with the most significant decreases occurring in the temporal-parietal region and hippocampus

[13]. Researchers have used a variety of animal models to simulate human CCH. BCCAO is characterized by continuous low CBF and can reasonably simulate dementia and age-related diseases caused by CCH in humans [14]. To approximate the status of human CCH, a rat BCCAO model was employed. A decrease in CBF was observed in the rats, reaching 50% at 1-2 weeks post-operation. Thereafter, a gradual return to the baseline level was noted at 4 weeks, which was attributed to the establishment of collateral circulation. Pathologic damage to rat brain tissue was observed and confirmed by H&E and Nissl staining. Behavioral experiments 4 weeks after surgery revealed a decrease in spatial memory, anxiety and depression-like behavior in the rats. In light of the aforementioned evidence, it can be reasonably concluded that the VCI rat model was successfully established.

Oxidative stress is a process in which an imbalance between antioxidants and pro-oxidants leads to oxidative damage to cellular proteins, lipids, and nucleic acids [15]. Due to the energy imbalance of CCH, ROS can be generated from multiple sources, including the electron transport chain, nicotinamide adenine dinucleotide phosphate oxidase (Nox), and nitric oxide synthase [16]. The primary cause of cognitive decline in CCH patients is increased oxidative stress in the central nervous system, which has a major effect on VCI, AD, and neurodegeneration [17, 18]. For example, elevated levels of the lipid peroxidation marker malondialdehyde (MDA) have been found in the cerebrospinal fluid of VCI and AD patients [19]. Of course, there are similar manifestations in CCH model rats: levels of the antioxidant GSH decrease, levels of the oxidant MDA increase, and these changes are closely related to cognitive dysfunction in rats [20]. Consistent with the study, decreased GSH expression and increased MDA expression were detected in the hippocampus of rats with CCH. According to these results, the hippocampus of rodents with CCH was damaged by oxidative stress. Pyroptosis is a type of cell death controlled by the release of various inflammatory cytokines. The classical pyroptosis pathway is mediated by the NLRP3 inflammasome, which is complemented by the caspase-1 and gasdermin protein families [21]. Neurologic disorders such as AD, traumatic brain injury (TBI), and cerebral ischemia-reperfusion injury have been associated with pyroptosis mediated by the NLRP3 inflammasome [22-24]. CCH may activate the NLRP3 inflammasome signaling pathway, which is involved in neuronal damage and synaptic damage, leading to cognitive dysfunction [25]. Matsuyama et al. also reported that activation of the NLRP3 and AIM2 inflammasomes and activation of the caspase-1 and GSDMD-mediated typical pyroptosis pathways were observed in CCH animal models [26]. Consistent with the study, western blotsdemonstrated elevated levels of pyroptosis-associated proteins, including NLRP3, caspase-1 cleavage, GSDMD-NT, and IL-1β in the CCH model.

TIGAR can protect mouse neurons from ischemia/reperfusion injury by reducing ROS levels [27]. It was noteworthy that TIGAR exhibited high expression levels in the hippocampus of rats with CCH. The discovery aligned with prior research indicating that elevated TIGAR expression in the mouse brain after ischemia/reperfusion was unrelated to TP53 and linked to heightened levels of ROS [28]. It was postulated that the observed increase in TIGAR levels in the CCH rat model may be associated with the positive feedback regulation stimulated by ROS accumulation. Although TIGAR could be highly expressed in hypoxic-ischemic brains, its expression increased 3-4 weeks after BCCAO. This suggests that the elevation in TIGAR may manifest at a late stage, with the oxidative stress injury to brain tissue occurring in the initial phase of CCH and subsequently becoming more pronounced. Therefore, the increase in endogenous TIGAR in the brain was not enough to alleviate CCH-induced nerve injury. Accordingly, the objective was to maintain a high level of TIGAR expression in the hippocampus prior to BCCAO in order to investigate the protective effect in the CCH rat model.

TIGAR enhanced the antioxidant capacity of cells by promoting the pentose phosphate pathway (PPP) and played a protective role in rat models of CCH. Activation of the PPP increased NADPH production, which is essential for maintaining GSH levels and reducing ROS accumulation. In addition, TIGAR reduced pyrodeath by inhibiting the activation of NLRP3, which may be achieved by reducing the production of ROS. Although this study did not directly examine the effects of TIGAR on Bcl-2 family

proteins, previous studies suggested that TIGAR could inhibit apoptosis by regulating these proteins. Therefore, TIGAR could protect neurons by regulating metabolic pathways and inhibiting inflammatory responses.

Numerous studies have shown that elimination or reduction of endogenous ROS production has neuroprotective effects [29, 30]. When the brain is damaged by ischemia and hypoxia, glucose metabolism in neurons is mainly glycolysis and the PPP is closed, resulting in a significant decrease in NADPH levels, which leads to a decrease in the antioxidant capacity of neurons [31]. TIGAR has enzymatic functions, mainly by blocking glycolysis and redirecting substrate flow to the PPP, thereby producing sufficient NADPH for antioxidant enzymes, maintaining reduced GSH, reducing ROS production, and playing a protective role in a variety of neurological diseases [32, 33]. After overexpression of TIGAR in the bilateral hippocampus of rats with CCH, the MDA level decreased, and the expression of NADPH and GSH increased. Behavioral experiments showed that the cognitive function and anxiety and depression-like behavior of the rats were improved. It is postulated that the reduction in oxidative stress may be associated with the behavioral enhancement observed in rats following TIGAR overexpression. An AD investigation demonstrated that overexpression of TIGAR could prevent pyroptosis [34]. In a CCH rat model, the overexpression of TIGAR was observed to exert an antipyroptotic effect, accompanied by a reduction in the expression of proteins linked to pyroptosis. Pathology revealed a higher survival rate of neurons, and TEM also revealed the formation of GSDMD membrane holes in hippocampal neurons. Uncertainty surrounds the antipyroptotic mechanism of TIGAR, which may be related to the reduction of ROS. mtDNA oxidation (ox-mtDNA) or ROS can activate the NLRP3 inflammasome [35]. Lipid peroxidation enhances the activity of GSDMD, promotes the binding of GSDMD-NT to the plasma membrane, and mediates an increase in cell mortality [36].

This study investigated the expression of NLRP3 and IL-1β in a CCH model and correlated them with the occurrence of pyroptosis. However, activation of NLRP3 does not always caused pyroptosis, and in some cases could induce only a low level of inflammatory response without causing cell membrane rupture. In addition, IL-1β is a common pro-inflammatory cytokine whose release is closely related to immune regulation and tissue repair and does not necessarily trigger cell lysis. Although this study was not able to include other pyroptosis-specific markers, these observations still provided valuable information on the inflammatory response under CCH conditions. Future studies will consider adding other markers related to pyrodeath to improve the specificity of detection and further confirm the role of pyrodeath in CCH.

In light of the current research findings, future studies will examine whether oxidative stress and pyroptosis are augmented following TIGAR knockdown and whether TIGAR exerts an influence on the behavior of rats with CCH. This study confirmed the antipyroptotic effect of TIGAR in rats with CCH, and further research is needed to confirm the specific signaling pathway involved and the effects of their specific inhibitors.

Conclusions

The results showed that oxidative stress and pyroptosis were activated in the hippocampus of rats with CCH. High levels of TIGAR help protect neurons from CCH-induced cognitive impairment by inhibiting oxidative stress and pyroptosis. These findings suggest that this molecule may be a novel therapeutic target for the prevention and treatment of CCH.

Disclosure of conflict of interest

None.

Address correspondence to: Bihua Wu, Apartment of Internal Medicine, Nanchong Mental Health Center, Nanchong 637000, Sichuan, China. E-mail: bhua100@163.com

References

[1] Skrobot OA, Black SE, Chen C, DeCarli C, Erkinjuntti T, Ford GA, Kalaria RN, O'Brien J, Pantoni L, Pasquier F, Roman GC, Wallin A, Sachdev P, Skoog I; VICCCS group, Ben-Shlomo Y, Passmore AP, Love S and Kehoe PG. Progress toward standardized diagnosis of vascular cognitive impairment: Guidelines from the vascular impairment of cognition classification consensus study. Alzheimers Dement 2018; 14: 280-292.

[2] Yu W, Li Y, Hu J, Wu J and Huang Y. A study on the pathogenesis of vascular cognitive impairment and dementia: the chronic cerebral hypoperfusion hypothesis. J Clin Med 2022; 11: 4742.
[3] Du SQ, Wang XR, Xiao LY, Tu JF, Zhu W, He T and Liu CZ. Molecular mechanisms of vascular dementia: what can be learned from animal models of chronic cerebral hypoperfusion? Mol Neurobiol 2017; 54: 3670-3682.
[4] Zhang Y, Zhang J, Zhao Y, Zhang Y, Liu L, Xu X, Wang X and Fu J. ChemR23 activation attenuates cognitive impairment in chronic cerebral hypoperfusion by inhibiting NLRP3 inflammasome-induced neuronal pyroptosis. Cell Death Dis 2023; 14: 721.
[5] Tan LL, Jiang XL, Xu LX, Li G, Feng CX, Ding X, Sun B, Qin ZH, Zhang ZB, Feng X and Li M. TP53-induced glycolysis and apoptosis regulator alleviates hypoxia/ischemia-induced microglial pyroptosis and ischemic brain damage. Neural Regen Res 2021; 16: 1037-1043.
[6] Zhaolin Z, Guohua L, Shiyuan W and Zuo W. Role of pyroptosis in cardiovascular disease. Cell Prolif 2019; 52: e12563.
[7] Bensaad K, Tsuruta A, Selak MA, Vidal MN, Nakano K, Bartrons R, Gottlieb E and Vousden KH. TIGAR, a p53-inducible regulator of glycolysis and apoptosis. Cell 2006; 126: 107-120.
[8] Li M, Sun M, Cao L, Gu JH, Ge J, Chen J, Han R, Qin YY, Zhou ZP, Ding Y and Qin ZH. A TIGAR-regulated metabolic pathway is critical for protection of brain ischemia. J Neurosci 2014; 34: 7458-7471.
[9] Guo J, Zhou M, Zhao M, Li S, Fang Z, Li A and Zhang M. TIGAR deficiency induces caspase-1-dependent trophoblasts pyroptosis through NLRP3-ASC inflammasome. Front Immunol 2023; 14: 1114620.
[10] Farkas E, Luiten PG and Bari F. Permanent, bilateral common carotid artery occlusion in the rat: a model for chronic cerebral hypoperfusion-related neurodegenerative diseases. Brain Res Rev 2007; 54: 162-180.
[11] Ciacciarelli A, Sette G, Giubilei F and Orzi F. Chronic cerebral hypoperfusion: an undefined, relevant entity. J Clin Neurosci 2020; 73: 8-12.
[12] Duncombe J, Kitamura A, Hase Y, Ihara M, Kalaria RN and Horsburgh K. Chronic cerebral hypoperfusion: a key mechanism leading to vascular cognitive impairment and dementia. Closing the translational gap between rodent models and human vascular cognitive impairment and dementia. Clin Sci (Lond) 2017; 131: 2451-2468.
[13] Dash S, Agarwal Y, Jain S, Sharma A and Chaudhry N. Perfusion CT imaging as a diagnostic and prognostic tool for dementia: prospective case-control study. Postgrad Med J 2022; 99: 318-325.
[14] Venkat P, Chopp M and Chen J. Models and mechanisms of vascular dementia. Exp Neurol 2015; 272: 97-108.
[15] Liu H and Zhang J. Cerebral hypoperfusion and cognitive impairment: the pathogenic role of vascular oxidative stress. Int J Neurosci 2012; 122: 494-499.
[16] Rajeev V, Chai YL, Poh L, Selvaraji S, Fann DY, Jo DG, De Silva TM, Drummond GR, Sobey CG, Arumugam TV, Chen CP and Lai MKP. Chronic cerebral hypoperfusion: a critical feature in unravelling the etiology of vascular cognitive impairment. Acta Neuropathol Commun 2023; 11: 93.
[17] Luca M, Luca A and Calandra C. The role of oxidative damage in the pathogenesis and progression of Alzheimer's disease and vascular dementia. Oxid Med Cell Longev 2015; 2015: 504678.
[18] Zhao Y and Gong CX. From chronic cerebral hypoperfusion to Alzheimer-like brain pathology and neurodegeneration. Cell Mol Neurobiol 2015; 35: 101-110.
[19] Aquilani R, Cotta Ramusino M, Maestri R, Iadarola P, Boselli M, Perini G, Boschi F, Dossena M, Bellini A, Buonocore D, Doria E, Costa A and Verri M. Several dementia subtypes and mild cognitive impairment share brain reduction of neurotransmitter precursor amino acids, impaired energy metabolism, and lipid hyperoxidation. Front Aging Neurosci 2023; 15: 1237469.
[20] Yan N, Xu Z, Qu C and Zhang J. Dimethyl fumarate improves cognitive deficits in chronic cerebral hypoperfusion rats by alleviating inflammation, oxidative stress, and ferroptosis via NRF2/ARE/NF-κB signal pathway. Int Immunopharmacol 2021; 98: 107844.
[21] Zhang L, Hu Z, Li Z and Lin Y. Crosstalk among mitophagy, pyroptosis, ferroptosis, and necroptosis in central nervous system injuries. Neural Regen Res 2024; 19: 1660-1670.
[22] Han C, Yang Y, Guan Q, Zhang X, Shen H, Sheng Y, Wang J, Zhou X, Li W, Guo L and Jiao Q. New mechanism of nerve injury in Alzheimer's disease: β-amyloid-induced neuronal pyroptosis. J Cell Mol Med 2020; 24: 8078-8090.
[23] Yang F, Li G, Lin B and Zhang K. Gastrodin suppresses pyroptosis and exerts neuroprotective effect in traumatic brain injury model by inhibiting NLRP3 inflammasome signaling pathway. J Integr Neurosci 2022; 21: 72.
[24] Xia P, Marjan M, Liu Z, Zhou W, Zhang Q, Cheng C, Zhao M, Tao Y, Wang Z and Ye Z. Chrysophanol postconditioning attenuated cerebral ischemia-reperfusion injury induced NLRP3-related pyroptosis in a TRAF6-dependent manner. Exp Neurol 2022; 357: 114197.
[25] Poh L, Sim WL, Jo DG, Dinh QN, Drummond GR, Sobey CG, Chen CL, Lai MKP, Fann DY and

Arumugam TV. The role of inflammasomes in vascular cognitive impairment. Mol Neurodegener 2022; 17: 4.
[26] Matsuyama H, Shindo A, Shimada T, Yata K, Wakita H, Takahashi R and Tomimoto H. Chronic cerebral hypoperfusion activates AIM2 and NLRP3 inflammasome. Brain Res 2020; 1736: 146779.
[27] Chen J, Zhang DM, Feng X, Wang J, Qin YY, Zhang T, Huang Q, Sheng R, Chen Z, Li M and Qin ZH. TIGAR inhibits ischemia/reperfusion-induced inflammatory response of astrocytes. Neuropharmacology 2018; 131: 377-388.
[28] Cao L, Chen J, Li M, Qin YY, Sun M, Sheng R, Han F, Wang G and Qin ZH. Endogenous level of TIGAR in brain is associated with vulnerability of neurons to ischemic injury. Neurosci Bull 2015; 31: 527-40.
[29] Radi E, Formichi P, Battisti C and Federico A. Apoptosis and oxidative stress in neurodegenerative diseases. J Alzheimers Dis 2014; 42 Suppl 3: S125-S152.
[30] Jiang P, Chen L, Sun J, Li J, Xu J, Liu W, Feng F and Qu W. Chotosan ameliorates cognitive impairment and hippocampus neuronal loss in experimental vascular dementia via activating the Nrf2-mediated antioxidant pathway. J Pharmacol Sci 2019; 139: 105-111.
[31] Bélanger M, Allaman I and Magistretti PJ. Brain energy metabolism: focus on astrocyte-neuron metabolic cooperation. Cell Metab 2011; 14: 724-738.
[32] Tang J, Chen L, Qin ZH and Sheng R. Structure, regulation, and biological functions of TIGAR and its role in diseases. Acta Pharmacol Sin 2021; 42: 1547-1555.
[33] Huang B, Lang X and Li X. The role of TIGAR in nervous system diseases. Front Aging Neurosci 2022; 14: 1023161.
[34] Lei B, Liu J, Yao Z, Xiao Y, Zhang X, Zhang Y and Xu J. NF-κB-Induced upregulation of miR-146a-5p promoted hippocampal neuronal oxidative stress and pyroptosis via TIGAR in a model of Alzheimer's disease. Front Cell Neurosci 2021; 15: 653881.
[35] Xian H, Watari K, Sanchez-Lopez E, Offenberger J, Onyuru J, Sampath H, Ying W, Hoffman HM, Shadel GS and Karin M. Oxidized DNA fragments exit mitochondria via mPTP- and VDAC-dependent channels to activate NLRP3 inflammasome and interferon signaling. Immunity 2022; 55: 1370-1385, e8.
[36] Weindel CG, Ellzey LM, Martinez EL, Watson RO and Patrick K. Gasdermins gone wild: new roles for GSDMs in regulating cellular homeostasis. Trends Cell Biol 2023; 33: 773-787.